

Targeting the binding pocket of the fluorophore 8-anilidonaphthalene-1-sulfonic acid in the bacterial enzyme MurA

Reem K. Fathalla | Matthias Engel  | Christian Ducho 

Department of Pharmacy, Pharmaceutical and Medicinal Chemistry, Saarland University, Saarbrücken, Germany

Correspondence

Matthias Engel and Christian Ducho, Department of Pharmacy, Pharmaceutical and Medicinal Chemistry, Saarland University, Campus C2 3, 66 123 Saarbrücken, Germany. Email: ma.engel@mx.uni-saarland.de and christian.ducho@uni-saarland.de

Funding information

None

Abstract

8-Anilidonaphthalene-1-sulfonic acid (ANS) has been extensively used as a fluorescent probe to detect conformational changes of proteins. It has been cocrystallized with several of the proteins it is used to monitor, including the bacterial cell wall synthesis enzyme MurA. MurA catalyzes the first committed step of peptidoglycan biosynthesis, converting UDP-*N*-acetylglucosamine (UDP-GlcNAc) into enolpyruvyl UDP-GlcNAc. It has been reported before that ANS binds to MurA from *Enterobacter cloacae* without inhibiting the enzyme's activity up to a concentration of 1 mM ANS. In this study, we present evidence that ANS inhibits the activity of several isoforms of MurA with IC₅₀ values of 18, 22, and 31 μM against wild-type *Escherichia coli*, C115D *E. coli*, and *E. cloacae* MurA, respectively. This prompted us to test a larger series of structural analogs of ANS for the inhibition of these MurA enzymes, which led to the discovery of compound **26**. This ANS analog showed enhanced inhibition of MurA (WT and C115D MurA from *E. coli*, and *E. cloacae* MurA) with IC₅₀ values of 2.7, 10, and 14 μM, respectively. Based on our results, the ANS binding pocket was identified as a novel target site for the development of potential antibiotics.

KEYWORDS

ANS, fluorescence binding assay, MurA, peptidoglycan biosynthesis, sulfonic acids

1 | INTRODUCTION

The fluorescent dye 8-anilidonaphthalene-1-sulfonic acid (ANS, Figure 1) has historically been used as a probe to monitor various proteins, as it shows little to no fluorescence in aqueous environment, but the fluorescence is greatly enhanced with a green-to-blue shift when the compound is bound to proteins.^[1–3] ANS is able to bind to the hydrophobic pockets of proteins to detect molten globules, ligand binding, nonpolar patches on the surface of proteins, protein

aggregation, and general conformational changes.^[4–10] Its binding to proteins has been attributed to its ability to form hydrophobic interactions through its anilidonaphthalene core in addition to binding to the cationic side chains of proteins via its sulfonic acid moiety.^[4,10,11] The binding affinities are usually low though, with reported *K_d* values ranging from 37 μM (CDK2) to 83 μM (bovine serum albumin).^[12,13] Nevertheless, several X-ray crystal structures of ANS in complex with a number of proteins are available, such as S100A7,^[14] human heart fatty acid binding protein,^[15] CDK2,^[13] and

This is an open access article under the terms of the Creative Commons Attribution-NonCommercial-NoDerivs License, which permits use and distribution in any medium, provided the original work is properly cited, the use is non-commercial and no modifications or adaptations are made.

© 2023 The Authors. *Archiv der Pharmazie* published by Wiley-VCH GmbH on behalf of Deutsche Pharmazeutische Gesellschaft.

Ppm1p,^[16] in addition to the reported complex of ANS with the bacterial cell wall synthesis enzyme MurA.^[3]

MurA is the first enzyme in the bacterial peptidoglycan biosynthesis pathway. It catalyzes the transfer of an enolpyruvate moiety from phosphoenolpyruvate (PEP) to UDP-*N*-acetylglucosamine (UDP-GlcNAc, UNAG) (Scheme 1).^[3,17–19] Heterologously overexpressed MurA is usually isolated in a closed conformation with a PEP molecule covalently bound to the Cys115 residue and having UDP-*N*-acetylmuramic acid (UDP-MurNAc) noncovalently bound to its active site. UDP-MurNAc is the product of the MurB-catalyzed reaction, that is, the next step in peptidoglycan biosynthesis after the MurA-mediated transformation.^[19–24] This closed conformation is extremely robust to dilution and most commonly used salts in protein purification and crystallization. However, it can be unlocked using the natural MurA substrate UDP-GlcNAc or the side product of the enzymatic reaction, inorganic phosphate (P_i).^[20]

Fosfomycin (compound I, Figure 2) is the only clinically used antibiotic targeting MurA.^[25,26] It inactivates the enzyme by irreversibly binding to the catalytically important Cys115 residue.^[17,27,28] However, emerging fosfomycin resistance among clinical isolates from diverse bacterial pathogens has been reported.^[29–33] The naturally occurring C115D MurA mutant present in Mycobacteria is resistant to inhibition by fosfomycin.^[22] Other mechanisms of fosfomycin resistance include decreased uptake,^[33,34] enzymatic modification of the antibiotic,^[35,36] and finally, MurA overexpression.^[37,38] There is a variety of previously reported MurA inhibitors such as the sesquiterpene lactone derivative cnicin,^[39,40] aminotetralones,^[41] benzoxathiolone derivatives,^[42] bromo-nitrovinylfuran,^[43] and avenaciolides^[44] (compounds II–VI, respectively,

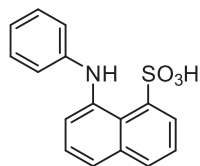
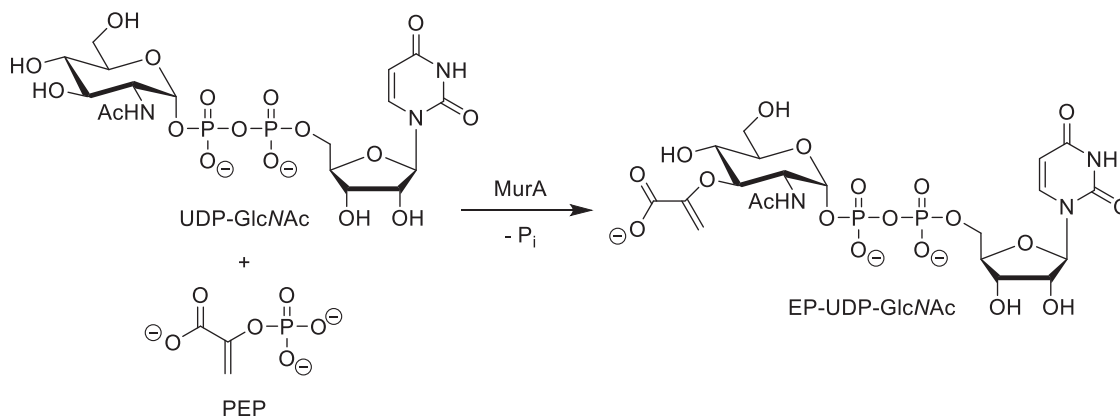


FIGURE 1 Structure of 8-anilino-1-naphthalenesulfonic acid (ANS).



SCHEME 1 MurA-catalyzed reaction.

Figure 2). These inhibitors, while often potent toward MurA to a significant extent, show a multitude of limitations that hamper their development into viable drug candidates. These shortcomings include resistance of the C115D MurA mutant (for compounds II–IV),^[40–42] nonspecific target inhibition and thus cellular toxicity (compounds V and VI),^[43,45] and general interaction with thiols in proteins or compounds such as glutathione (GSH) (compounds IV and V).^[42,43]

ANS has been used as a fluorescent probe to monitor the conformational changes that occur during binding events of MurA using a corresponding binding assay.^[24,46,47] These experiments have mainly been performed using *Enterobacter cloacae* MurA, for which it was reported that ANS did not show any inhibition of the bacterial enzyme up to a 1 mM concentration.^[47] An X-ray cocrystal structure of *E. cloacae* MurA bound to ANS is available (PDB code 1EYN), showing that the anilino-naphthalene core is engaged in interactions with Arg91, Pro112, and Gly113, while the sulfonic acid moiety forms an H-bond to Gly113 and captures the active site loop residue Arg120 through a salt bridge (Figure 3).^[3] In the enzyme-substrate complex, both Arg91 and Arg120 interact with the diphosphate bridge of the substrate UDP-GlcNAc,^[19] and Arg120 has further roles in the catalytic mechanism.^[20] We therefore hypothesized that binding of ANS might stabilize an inactive conformation of MurA that would be incapable of substrate binding and catalyzing the enolpyruvate transfer.

In this work, we report that ANS and some ANS-derived naphthyl sulfonic acids actually showed inhibition of wild-type (WT) and C115D *Escherichia coli* MurA, in addition to *E. cloacae* MurA. The small size of these inhibitors affords them remarkable ligand efficiency, and their facile availability allowed us to efficiently explore their structure–activity relationship (SAR).

2 | RESULTS AND DISCUSSION

2.1 | Chemistry

All the initially tested compounds were commercially available, simplified derivatives of ANS lacking the *N*-phenyl group, that is, in

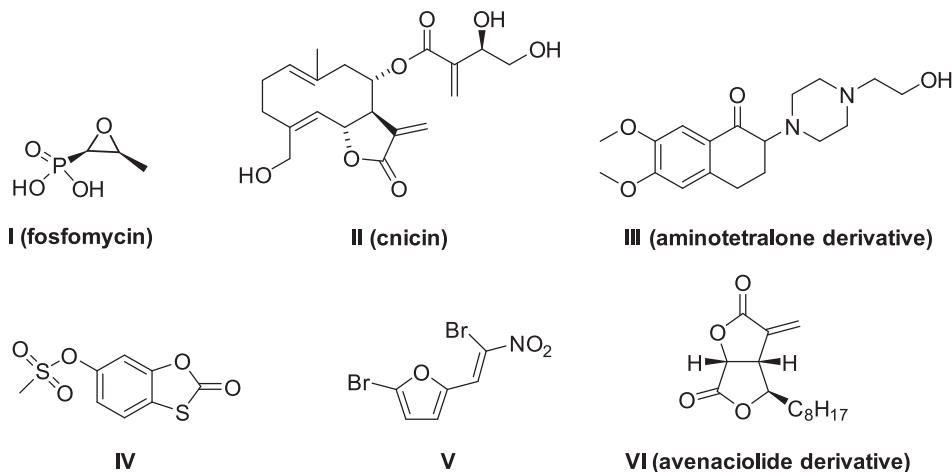


FIGURE 2 Previously reported MurA inhibitors.

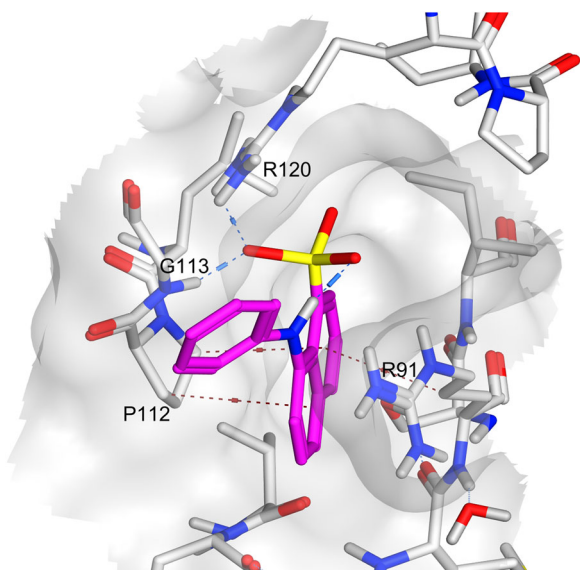


FIGURE 3 Structural representation of the binding of 8-anilino-1-naphthalene-sulfonic acid (ANS) (magenta sticks) to its binding pocket in MurA based on the reported X-ray cocrystal structure (PDB: 1EYN).^[3] The figure shows CH- π interactions (in brown) between the aminonaphthalene core and the two residues Arg91 and Pro112. The sulfonic acid moiety forms a salt bridge with Arg120 and an H-bond with the Gly113 backbone NH (electrostatic interactions in blue). In addition, the guanidine unit of Arg91 is close to the naphthalene and the face of the phenyl group for cation- π interactions.

most cases possessing both the sulfonic acid group and another functionality on the naphthalene ring. We started by studying benzene (**1**) and naphthalene sulfonic acids **2** and **3** as well as naphthalene acetic acid **4** in addition to several naphthols **5–9** (Table 1). The next step was to explore 1-naphthalene sulfonic acids with an amino group at different positions on the naphthalene ring (**10–14**, Table 2). Furthermore, replacing the amino group with a hydroxy group

was also studied (**15, 16**, Table 2). Finally, the effect of two sulfonic acid groups attached to the naphthalene scaffold in addition to amino and/or hydroxy groups was evaluated (**20–27**, Table 3).

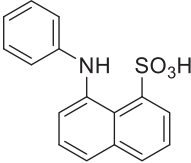
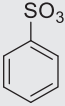
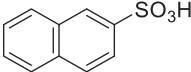
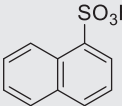
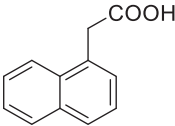
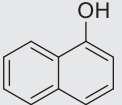
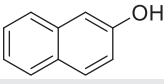
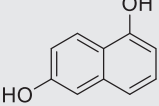
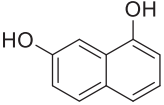
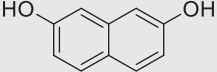
2.2 | Biological evaluation

2.2.1 | Initial compound selection and MurA inhibition

ANS was initially tested as an inhibitor of WT *E. coli* MurA, against which it showed 91% inhibition at 100 μ M. It also exhibited 83% and 97% inhibition against C115D *E. coli* and *E. cloacae* MurA, respectively. We initially tested small fragments **1–9** based on the structural features of ANS. They were either substructures of the parent compound, had acidic functions at different positions, or possessed hydroxyl groups as hydrogen bond donor/acceptor combinations. These selected compounds were also first tested against WT *E. coli* MurA at 100 μ M. Subsequently, for compounds showing 30% inhibition or more, the inhibitory potencies against C115D *E. coli* MurA and *E. cloacae* MurA were also measured. IC₅₀ values were determined for compounds showing more than 50% inhibition at 100 μ M (Table 1).

For this first stage of the SAR study, the sulfonic acid moiety was attached either to a benzene or a naphthalene ring at positions 1 and 2 (compounds **1–3**), revealing only minimal MurA inhibition by such fragments. It might be noteworthy though that the presence of the sulfonic acid at position 1 of the naphthalene ring (compound **3**) furnished a slightly better activity than the 2-regioisomer (compound **2**). The naphthyl acetic acid derivative (compound **4**) also did not show appreciable MurA inhibition. Naphthols **5–9** showed better MurA inhibition, but the inhibition was still not very strong, thus highlighting the relevance of the sulfonic acid group. Overall, none of the smaller fragments **1–9** retained the activity of ANS, indicating that the combination of additional structural motifs of ANS provided its activity.

TABLE 1 MurA inhibition of the first series of 8-anilidonaphthalene-1-sulfonic acid (ANS) analogs (1–9).

Compound	Structure	<i>Escherichia coli</i> wild-type (WT) MurA		<i>E. coli</i> C115D MurA		<i>Enterobacter cloacae</i> MurA	
		% inhibition @100 μ M	IC ₅₀ \pm SD (μ M)	% inhibition @100 μ M	IC ₅₀ \pm SD (μ M)	% inhibition @100 μ M	IC ₅₀ \pm SD (μ M)
ANS		91	18 \pm 4	83	22 \pm 8	97	31 \pm 3
1		0	n.d.	n.d.	n.d.	n.d.	n.d.
2		5	n.d.	n.d.	n.d.	n.d.	n.d.
3		17	n.d.	n.d.	n.d.	n.d.	n.d.
4		13	n.d.	n.d.	n.d.	n.d.	n.d.
5		34	n.d.	11	n.d.	6	n.d.
6		36	n.d.	7	n.d.	3	n.d.
7		22	n.d.	n.d.	n.d.	n.d.	n.d.
8		19	n.d.	n.d.	n.d.	n.d.	n.d.
9		28	n.d.	n.d.	n.d.	n.d.	n.d.

Note: n.d. = not determined with respect to low inhibition against *E. coli* WT MurA at 100 μ M.

For the next stage of the SAR study, we chose compounds with closer structural resemblance to ANS, having a sulfonic acid group and a hydrogen bond donor (NH₂ or OH) at various positions of the naphthalene rings (Table 2). Compounds 10–13 had the sulfonic acid moiety at position 1 of the naphthalene scaffold in addition to an amino group at various positions. They were generally active against *E. cloacae* MurA. At the same time, only compounds 11 and 13 were reasonably active against both WT and C115D *E. coli* MurA, with 11 (the 5-amino derivative) having an IC₅₀ value of 9.0 μ M against WT *E. coli* MurA. Compound 13, differing from ANS by the missing phenyl unit at the 8-amino group, exhibited only part of the activity of ANS, confirming that the phenyl moiety contributed to the binding affinity, probably by interacting with Arg131 (Figure 3).

Thus, 11 was the most potent compound identified so far and was active against all three studied MurA isoforms. When the position of the sulfonic acid group of 11 was formally shifted from 1-sulfonate to 2-sulfonate in 14, a decrease in *E. coli* MurA inhibition was observed. However, activity against *E. cloacae* MurA was retained. In compounds 15 and 16, the 5- and 8-amino groups of compounds 11 and 13, respectively, were changed to hydroxy groups. This led to significantly decreased activities against all three MurA homologs, with only compound 15 showing some inhibition of WT *E. coli* MurA. Having two hydrogen bond donor moieties in compounds 17 and 18 was not favorable for the inhibitory activities. The added steric bulk or disadvantageous influence of the positive charge of the benzylic amino group of compound 18 decreased the

TABLE 2 MurA inhibition of the second series of 8-anilidonaphthalene-1-sulfonic acid (ANS) analogs (10–19).

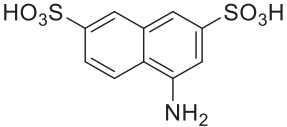
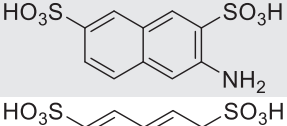
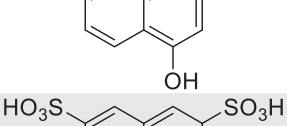
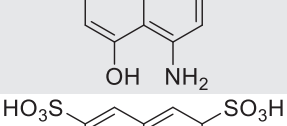
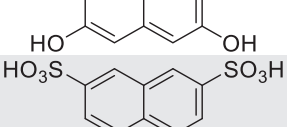
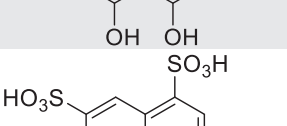
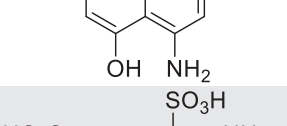
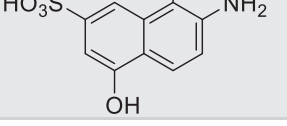
Compound	Structure	<i>Escherichia coli</i> wild-type (WT) MurA		<i>E. coli</i> C115D MurA		<i>Enterobacter cloacae</i> MurA	
		% inhibition @100 μ M	IC ₅₀ \pm SD (μ M)	% inhibition @100 μ M	IC ₅₀ \pm SD (μ M)	% inhibition @100 μ M	IC ₅₀ \pm SD (μ M)
10		48	n.d.	8	n.d.	64	49 \pm 5
11		95	9.0 \pm 0.3	78	18 \pm 3	95	31 \pm 2
12		31	n.d.	48	n.d.	61	31 \pm 3
13		66	44 \pm 10	54	46 \pm 2	42	n.d.
14		40	n.d.	0	n.d.	66	27 \pm 3
15		82	45 \pm 11	48	n.d.	12	n.d.
16		38	n.d.	12	n.d.	4	n.d.
17		46	n.d.	49	n.d.	33	n.d.
18		24	n.d.	n.d.	n.d.	n.d.	n.d.
19		39	n.d.	48	n.d.	61	44 \pm 3

Note: n.d. = not determined with respect to low inhibition against *E. coli* WT MurA at 100 μ M.

activity, as is evident from the comparison with **10**. Replacing the 1-sulfonic acid moiety of compound **11** with a carboxylic group in compound **19** led to a significant loss in potency particularly in the case of both *E. coli* MurA isoforms, clearly indicating that the

tetrahedral sulfonic acid group cannot be replaced by the planar carboxylic acid function. This is in full agreement with the spatial arrangement of the multiple electrostatic interactions of the sulfonic acid group in the ANS-MurA cocrystal structure (Figure 3).

TABLE 3 MurA inhibition of the third series of 8-anilidonaphthalene-1-sulfonic acid (ANS) analogs (20–27).

Compound	Structure	<i>Escherichia coli</i> wild-type (WT) MurA		<i>E. coli</i> C115D MurA		<i>Enterobacter cloacae</i> MurA	
		% inhibition @100 μ M	IC ₅₀ \pm SD (μ M)	% inhibition @100 μ M	IC ₅₀ \pm SD (μ M)	% inhibition @100 μ M	IC ₅₀ \pm SD (μ M)
20		96	9.1 \pm 0.6	5	n.d.	57	39 \pm 10
21		94	5.0 \pm 2.4	70	56 \pm 3	81	33 \pm 8
22		82	51 \pm 5	38	n.d.	22	n.d.
23		97	6.2 \pm 0.4	88	33 \pm 8	92	24 \pm 2
24		54	84 \pm 9	56	85 \pm 9	6	n.d.
25		99	0.95 \pm 0.23	87	31 \pm 5	49	n.d.
26		96	2.7 \pm 0.5	95	10 \pm 2	93	14 \pm 1
27		98	11 \pm 1	84	26 \pm 5	66	89 \pm 6

Note: n.d. = not determined with respect to low inhibition against *E. coli* WT MurA at 100 μ M.

Finally, a third stage of SAR studies involved testing of compounds having two sulfonic acid groups in addition to the hydrogen bond-forming moieties (Table 3). As a first set of according potential MurA inhibitors, 2,7-disulfonic acid derivatives having one or two additional hydrogen bond-forming units were tested (compounds 20–25). In general, these compounds were strongly active against all studied MurA homologs, indicating a beneficial effect of the extra sulfonic acid group in the structure. However, there were two notable exceptions from this trend. First, for compounds 20 and 22, a marked drop in activity was observed with the C115D mutant relative to WT *E. coli* MurA. A possible explanation could be that the inhibitory mechanism of these compounds involved covalent adduct formation with Cys115 in WT MurA, which would be impossible in the C115D mutant. However, molecular docking studies revealed such a covalent reaction to be highly unlikely though

(vide infra). Second, the hydroxy derivatives (compounds 22, 24, and 25) showed decreased activity against *E. cloacae* MurA, thus suggesting a limited tolerance of the *E. cloacae* enzyme toward the phenolic hydroxy group as a structural motif. This is particularly evident from 24 and 25, where the symmetric dihydroxy substitution does not allow placing the hydroxyl in a less detrimental binding orientation. Presumably, the higher electron density at the oxygen (relative to the amino nitrogen) might cause electrostatic repulsion with the backbone carbonyl of either Val87 or Lys88 at the bottom of the ANS binding pocket (cf. Figure 6), while an H-bond cannot form due to the unsuitable donor angle of the hydroxyl. Consistent with this hypothesis, the introduction of an amino group as a second hydrogen bonding motif on the naphthalene ring (compound 23) restored the inhibition of *E. cloacae* MurA, because the different angle of the amino function would allow H-bond formation with either the Val87

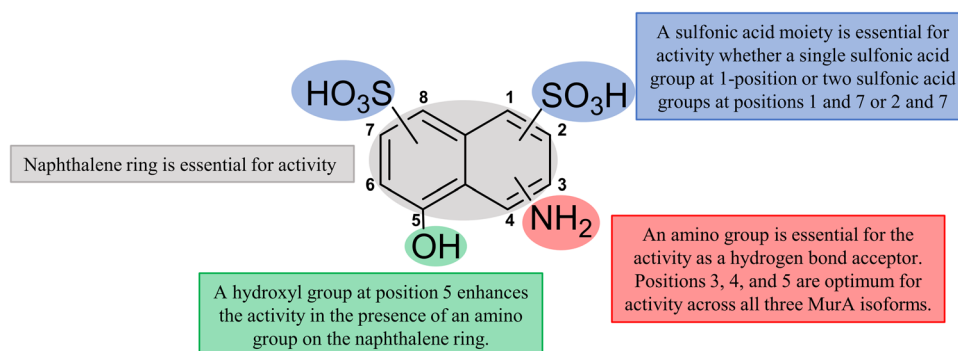


FIGURE 4 Summary of the structure–activity relationship (SAR) results of 8-anilino-1-naphthalene-1-sulfonic acid (ANS) derivatives for the inhibition of MurA.

backbone carbonyl or the Ser93 side chain (cf. Figure 6), thus positively contributing to the binding affinity.

Compounds **26** and **27** had the sulfonic acid moieties at positions 1 and 7 in addition to the presence of both amino and hydroxy groups. In particular for compound **26**, the favorable mixed amino/hydroxy substitution at the naphthalene scaffold was combined with the optimum placement of the second sulfonic acid group, thus furnishing the most potent compound against both C115D *E. coli* and *E. cloacae* MurA and the second most potent inhibitor of WT *E. coli* MurA. The overall resultant SAR for the inhibition of MurA by ANS and its analogs is summarized in Figure 4.

2.2.2 | Antibacterial activity

The compounds were tested as inhibitors of the growth of *E. coli* Δ tolC (an efflux-deficient *E. coli* strain) and *S. aureus* (Newman strain). All the tested compounds, including ANS, did not show any notable growth inhibition at concentrations up to 100 μ M. This finding might be attributed to the compounds' inability to enter the bacterial cells resulting from their highly polar nature with at least one sulfonic acid moiety in the structure.

2.2.3 | Fluorescence-based binding assay

A fluorescence-based binding assay was performed to confirm the binding of ANS and two of its derivatives (compounds **11** and **26**) to both WT *E. coli* and *E. cloacae* MurA (Figure 5). The concentration used for each compound was titrated according to the fluorescence intensity produced from measuring the respective compound alone. ANS had minimal fluorescence on its own, and thus a concentration of 100 μ M was used in the measurements. Compounds **11** and **26** had a fluorescence intensity that was higher than the detection limit of the spectrofluorometer at 100 μ M, and therefore, lower concentrations (10 μ M and 1 μ M for **11** and **26**, respectively) had to be used.

According to the model proposed by Kosower and Kanety,^[48] the marked solvatochromism of ANS is dependent on its 8-anilino

function, which adopts a more coplanar conformation in a nonpolar environment, thus allowing an electron transfer to the naphthalene ring system upon light excitation, followed by radiative relaxation. Since this anilino substituent was lacking in ANS analogs **11** and **26**, a similar increase in fluorescence intensity upon binding to a lipophilic protein pocket could not be expected with these derivatives. However, it was still conceivable that the intense fluorescence of their naphthalene ring systems could be quenched upon binding to the ANS pocket of MurA, in which the more lipophilic environment, but also the presence of potentially interacting H-bond donor/acceptor functions would modulate the electronic push–pull system created by the hydroxy/amino and sulfonic acid substituents.

In the reference experiment, ANS showed a weak fluorescence intensity in the absence of MurA that increased when bound to MurA after addition of the protein (Figure 5a). This was in agreement with previously reported results.^[47] The increase in ANS fluorescence intensity was significantly higher with *E. coli* MurA than with *E. cloacae* MurA. For compound **11**, no change in fluorescence was observed for the compound in the absence and presence of MurA (Figure 5b). However, for compound **26**, a quenching effect on the fluorescence was observed when the compound was bound to both MurA homologs (Figure 5c). Apparently, the type and positions of substituents in the naphthalene ring of **26** allowed interactions with the binding pocket that also led to a partial fluorescence quenching, whereas the different substitution patterns in **11** seemed unsuitable for coupling potential interactions of **11** in the binding site with its intrinsic fluorescence. Thus, the quenching effect observed for **26** clearly confirmed a binding event with both WT *E. coli* and *E. cloacae* MurA, even though the fluorescence assay was not generally applicable as a binding assay with the studied ANS analogs (as observed with **11**).

2.3 | Molecular docking

To derive a binding model for our most potent inhibitor **26**, it was straightforward to perform molecular docking to the ANS binding pocket from the X-ray cocrystal structure with *E. cloacae* MurA (PDB entry 1EYN).^[3] Although there was no comparable ANS cocrystal

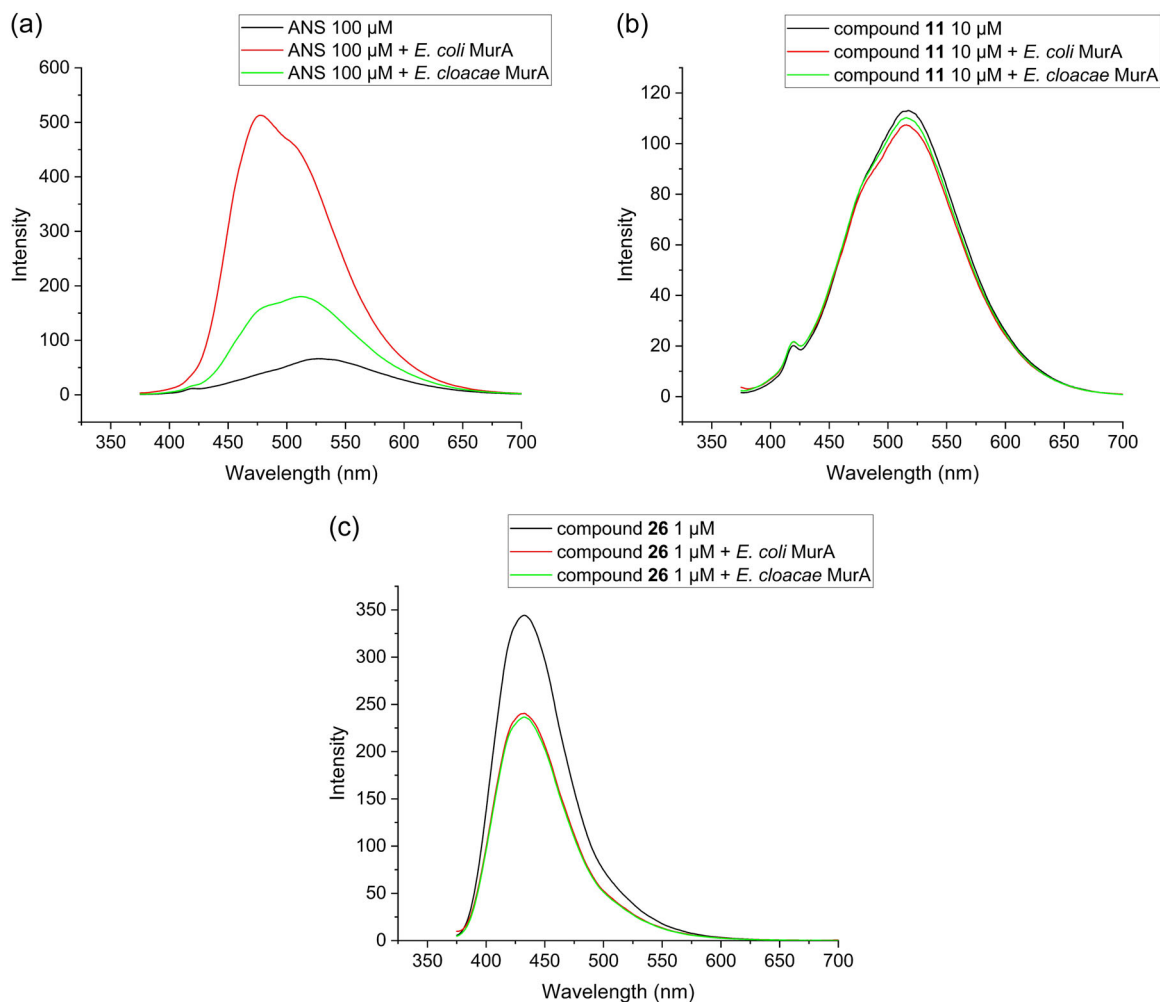


FIGURE 5 Results from the fluorescence-based binding assay with *Escherichia coli* MurA (red line) and *Enterobacter cloacae* MurA (green line) for: (a) 100 μM 8-anilinoanthracene-1-sulfonic acid (ANS). (b) 10 μM compound 11. (c) 1 μM compound 26.

structure with *E. coli* MurA available, it should be noted that all residues lining the ANS binding pocket are strictly conserved between the two species, suggesting that ANS and its derivatives may interact similarly with both MurA homologs.

In our model, the binding of compound 26 was mainly driven by electrostatic interactions, particularly by the salt bridges between the sulfonic acid moieties and Arg120 and Arg91, respectively (Figure 6a). Thus, the gain of potency observed with most derivatives carrying two sulfonic acid functions (Table 3) can be explained by the formation of a second salt bridge, in addition to the one already present with ANS (cf. Figure 3). Being exposed to the solvent, the sulfonic acid in position 1 may not only directly interact with Arg120, but also with Arg91 via a bridging water molecule. The predicted H-bonds of the 4-amino- and 5-hydroxy substituents with Ser93 and the Lys88 backbone carbonyl, respectively, are also in agreement with the obtained SAR data, as this mixed tandem motif enhanced the inhibitory potency (compare compounds 23 and 25, Table 3). Additional contributions to the binding affinity arise from the CH- π interactions between the naphthyl ring and Pro112/Arg91. The superimposition of the docking pose with ANS as bound in the

cocrystal structure shows that compound 26 was positioned in an overall similar manner, where the naphthyl ring and the 1-sulfonic acid largely overlap (Supporting Information: Figure S1). This was not surprising as the binding mode was mainly controlled by the optimal interaction with the arginine residues 91 and 120, both with ANS and 26. In the case of ANS, the 8-aminophenyl moiety is marginally engaged in a cation- π interaction with Arg91 (Figure 3), while for 26, Arg91 is captured by the 1-sulfonic acid. Overall, the rather small molecule 26 is densely decorated by substituents that are all involved in interactions with the binding pocket.

Eventually, the binding model as well as the cocrystal structure with ANS indicate that the ANS binding pocket extends into a hydrophobic groove, defined by the residues Val109, Leu111, Pro121, Val122, and Ile94 (Figure 6b), thus offering the advantageous possibility to significantly enhance the binding affinity through expansion of the ANS core toward that direction.

Compounds 20 and 22 had shown reduced inhibitory activity toward the C115D mutant relative to WT *E. coli* MurA, leading to the speculation that covalent adduct formation with Cys115 might be involved in the inhibition of WT MurA at least for some of the studied

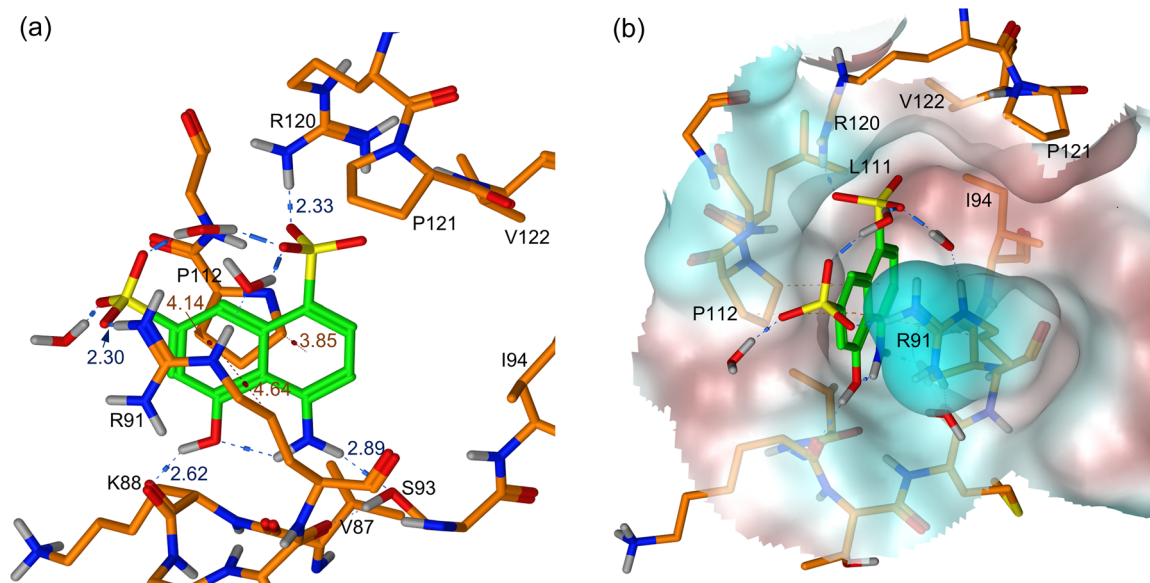


FIGURE 6 Predicted binding model of **26** in the 8-anilinoanthalene-1-sulfonic acid (ANS) binding pocket of *Enterobacter cloacae* MurA. Compound **26** (green) was docked in the binding pocket occupied by ANS in the X-ray cocrystal structure with MurA, using the PDB coordinates 1EYN.^[3] (a) Side view showing the predicted ionic, H-bond and CH- π interactions. Residues of interacting side chains and of the adjacent hydrophobic cluster are labeled, numbers denote ligand-protein distances in Å. (b) Top view with transparent Connolly surface encoding hydrophilic (cyan) and lipophilic (brown) areas. The interacting residues and the lipophilic residues within a 5.5 Å radius in the connected hydrophobic groove are labeled. Electrostatic interactions are indicated in blue and CH- π interactions in brown, the protein chain is colored orange. Some residues are omitted for clarity.

ANS-derived MurA inhibitors (vide supra). However, the molecular docking results strongly suggest that such a covalent reaction is highly unlikely, given the large distance between the Cys115 thiol and the nearest naphthalene carbon (9.4 Å, Supporting Information: Figure S2a) and the potential steric occlusion by the Leu111 side chain. Therefore, we investigated the potential reason for this difference using molecular docking simulations with **20**. To this end, the C115D mutation was introduced in silico into the ANS-bound MurA crystal structure (PDB entry 1EYN) using the “mutate” routine of MOE and the inbuilt rotamer library for aspartate. After energy minimization of the C115D mutant in the presence of ANS, ANS was replaced by **20** and the docking studies were carried out. In parallel, docking runs were performed with WT MurA (1EYN) using the same conditions.

In these studies, WT MurA consistently gave a complex in which **20** was bound by ionic interactions with both Arg91 and Arg120, several CH- π interactions and an H-bond between the amino function and the backbone carbonyl of Val87, thus resembling the binding mode predicted for the most potent compound **26** (Figure 6). In contrast, the presence of Asp115 instead of the cysteine unit created an alternative interaction motif for Arg120. Driven by electrostatic attraction, Asp115 was positioned in close proximity to Arg120 (Supporting Information: Figure S2b,c), thus competing with the sulfonate function of **20**. Hence, two principle types of binding poses were obtained. In the first set, an ionic interaction between Arg120 and the sulfonate moiety was observed, similarly to the complex with WT MurA. The Asp115 residue was still

considerably closer to Arg120 than the corresponding Cys115 in WT MurA (3.5 vs. 6.1 Å, respectively, Supporting Information: Figure S2a,b). In the alternative poses, Arg120 was engaged in a bidentate interaction with the Asp115 carboxylate and the carbonyl of Gly114, but did not form contacts with the sulfonate. These docking results suggested that in the C115D mutant, the flexible Arg120 may toggle between the sulfonate of **20** and Asp115/Gly114, leading to an overall reduction of binding affinity with **20** and other ANS analogs in which the sulfonates are placed in the 2- and 7-positions of the naphthalene scaffold. Only for these derivatives, Arg120 can bypass the sulfonate to reach Asp115.

3 | CONCLUSION

In this work, we have proven that the long-used fluorescent chemical probe ANS is actually an inhibitor of the bacterial protein MurA. This is in remarkable contrast to a previous report that had not found inhibitory activity of ANS toward MurA at concentrations up to 1 mM. In our experiments, ANS showed an IC₅₀ value of 17 μ M in vitro against WT MurA from *E. coli*. We also report SAR results for a series of ANS-derived naphthalene sulfonic acids that furnished MurA inhibitors with IC₅₀ values in the low micromolar range. They inhibited three different MurA isoforms including the fosfomycin-resistant C115D *E. coli* MurA, in addition to WT *E. coli* MurA and MurA from *E. cloacae*. The most potent overall inhibitor of all three MurA isoforms, compound **26**, had IC₅₀ values of 2.7, 10, and 14 μ M

on WT *E. coli*, C115D *E. coli*, and *E. cloacae* MurA, respectively. The docked binding mode of compound **26** shows that it interacts with MurA in a similar manner to ANS, while forming an extra salt bridge interaction with Arg 91, thus increasing its potency against MurA despite being smaller in size than ANS. These compounds did not inhibit bacterial growth, which may be attributed to poor cellular uptake resulting from their anionic properties. In the future, this issue might be solved by applying prodrug strategies for enhanced membrane permeation or by the replacement of the sulfonate units with boronic acid motifs. Our work shows that small ligands are able to efficiently inhibit MurA at low micromolar concentrations, as exemplified by compounds **23** and **26**. Thus, the ANS pocket could be classified as a druggable site that offers, besides the basic side chains, several H-bond donor/acceptor moieties, in addition to a yet unexploited adjacent hydrophobic groove lined by the side chains of Val109, Leu111, Pro121, Val122, and Ile94. Thus, it can be speculated that structurally extended ANS derivatives, addressing more of this potential interaction site, might well reach nM potencies. This extension of the parent structure may also help in improving the derivatives' physicochemical properties, thus facilitating their uptake into bacterial cells. ANS derivatives therefore represent new hit structures for the development of efficient MurA inhibitors with improved antibacterial potencies.

4 | EXPERIMENTAL

4.1 | Chemistry

All compounds were purchased from Sigma Aldrich, Alfa Aesar, BLD pharm, Carbosynth, Fluorochem, TCI, abcr, and AK Scientific and used as received (CAS numbers for the compounds are listed in Supporting Information: Table S1). The identity and purity of some selected relevant compounds was confirmed using LC-MS analysis (Supporting Information: Figures S3–S5). The InChI codes of the investigated compounds, together with some biological activity data, are provided as Supporting Information.

4.2 | Biological evaluation

4.2.1 | Cloning of the *murA* insert into an expression plasmid

The *E. cloacae murA* insert was obtained in a pEX-A258 vector from Eurofins Scientific (Supporting Information: Figure S6). The expression vector pGEX-4T-1 was obtained as part of the pGEX-4T-1-3xMyc-ERK2-K52R plasmid from Addgene. Both plasmids were double digested using 1 μ L each, NcoI and NotI restriction enzymes, and 5 μ L NEBuffer r3.1, all from New England Biolabs. One microgram of each plasmid was digested in a reaction with 50 μ L final volume, and the mixture was incubated at 37°C for 2 h. The resultant bands were purified using gel electrophoresis with a 1%

agarose gel in 1 \times TAE buffer (0.4 M Tris-acetate and 0.01 M EDTA). The samples were prepared as follows: for the reference 2 μ L pGOLD 1 kb DNA ladder was used in addition to 23 μ L water and 5 μ L 6 \times DNA loading dye (consisting of 25 mg bromothymol blue, 6 mL glycerol, and 4 mL 5 \times TAE buffer). As for the cut plasmids, to each 50 μ L reaction, 10 μ L 6 \times DNA loading dye was added. The samples were run at 100 V, and the gel was then incubated in 600 mL 1 \times TAE buffer and 30 μ L ethidium bromide for 30 min and then destained in water for 10 min. Bands of the correct size for the MurA insert and expression vector were cut (1291 and 5050 bp, respectively; Supporting Information: Figure S7). The DNA was extracted using the Macherey Nagel NucleoSpin Gel and PCR clean-up kit, with resultant concentrations being 7.8 ng/ μ L for the *E. cloacae* MurA insert and 13.5 ng/ μ L for the pGEX-4T1 vector. The insert and the vector were ligated with a ratio of 60 ng of the expression vector to 46 ng of the insert, according to the in silico University of Düsseldorf ligation calculator.^[49] One microliter T4 DNA ligase from New England Biolabs, 2 μ L 10 \times ligase buffer and water were added to a final volume of 20 μ L. The reaction was incubated at rt for 4 h and the ligated plasmid was used to transform chemically competent C41 *E. coli* BL21 cells.

4.2.2 | Transformation for overexpression of MurA

The bacterial transformation protocol started with thawing the competent C41 *E. coli* BL21 cells from Sigma Aldrich (catalog number CMC0017) on ice, then 50 ng plasmid DNA was added and the cells were incubated on ice for 30 min. The *E. coli* MurA WT and C115D mutant plasmids were obtained as previously described^[50] and the *E. cloacae* MurA expression plasmid was generated as described above. The cells were then heat-shocked for 1 min at 42°C and were again stored on ice for 2 min. Subsequently, 500 μ L LB medium was added to the cells and they were incubated at 37°C shaking at 180 rpm for 1 h in an INFORS HT Unitron shaking incubator. The cells were then plated on LB plates with 50 μ g/mL ampicillin and incubated at 37°C overnight. Plasmids were extracted from the produced cultures using the GenElute HP Plasmid Miniprep kit from Sigma Aldrich (catalog number PLN70). The purified plasmids were first checked by double-digestion using NcoI and NotI and applied to a 1% agarose gel (vide supra). The two bands with the correct masses of the insert and vector were observed (Figure S8, Supporting Information). They were then confirmed to have the correct sequence using DNA sequencing analysis by Azenta Life Sciences Inc. (predefined Sanger sequencing using 3GEX and 5GEX primers).

4.2.3 | Protein expression and purification

E. cloacae MurA was overexpressed as GST-tag fusion protein in *E. coli* BL21 cells. The transformed cells were grown at 37°C in LB medium (supplemented with 50 μ g/mL ampicillin) in the shaking incubator until a cell density (OD 600 nm) of 0.8 was reached (Thermo Fisher Scientific

Genesys 10uv spectrophotometer). The protein expression was then induced by the addition of 1 mM isopropyl β -D-1-thiogalactopyranoside (IPTG) with continued shaking at 37°C for 2 h. The cells were harvested by centrifugation at 4000 rpm and 4°C for 30 min. The resultant cell pellet was frozen at -80°C overnight to support cell lysis and maximize protein yield. The cell pellet was suspended in 10 mL lysis buffer consisting of 125 mM Tris-HCl (pH 7.5), 150 mM NaCl, 1 mM 1,4-dithio-D-threitol (DTT), 1 mM EDTA, 1 mg/mL lysozyme from chicken egg white, 0.5% Igepal (v/v), and a protease inhibitor cocktail tablet (Roche, cOmplete). Cells were then sonicated on ice for 10 min. The supernatant was obtained following centrifugation at 4000 rpm at 4°C for 30 min and then loaded onto PureCube Glutathione agarose beads and incubated at 4°C for 1 h in an end-to-end shaker for optimum binding. The beads were applied to disposable 5 mL polypropylene columns (Thermo Scientific) and three washing steps were performed using a wash buffer containing 125 mM Tris-HCl (pH 7.5), 150 mM NaCl, 1 mM DTT, and 1 mM EDTA. The GST-tagged protein was eluted using 125 mM Tris-HCl (pH 7.5), 150 mM NaCl, 1 mM DTT, in addition to 50 mM reduced glutathione. The resultant protein was dialyzed at 4°C against a buffer containing 20 mM Tris-HCl (pH 7.5), 150 mM NaCl, 1 mM DTT, protease inhibitor cocktail and 10% glycerol. The resultant protein concentration was 1.4 μ g/ μ L as determined using a Thermo Fisher Scientific NanoDrop 2000. The protein was then aliquoted, flash-frozen in liquid nitrogen, and stored at -80°C. *E. coli* K12 MurA and the C115D mutant enzymes were overexpressed as His-tag fusion proteins in *E. coli* BL21 cells according to a previously reported procedure.^[50]

4.2.4 | MurA assay

The assay was performed in 96-well plates (Greiner bio-one, F-bottom clear) in a final volume of 100 μ L. 1.25 μ g of WT *E. coli* MurA or 0.625 μ g *E. cloacae* MurA was preincubated with 150 μ M UNAG at rt for 15 min. Then the potential inhibitors dissolved in DMSO (or pure DMSO as a control) were added and the mixture was further incubated at rt for 15 min (total DMSO concentration 2%). A master mix consisting of 150 μ M PEP, 2 mM DTT and 25 mM Tris-HCl (pH 7.5, final concentrations) was then added and the mixture was incubated at 37°C for 30 min. In the case of *E. coli* C115D MurA, the initial UNAG preincubation step was skipped and the protein was directly preincubated with the inhibitors, while 150 μ M UNAG was added to the master mix. The reaction was stopped by the addition of 100 μ L of a solution containing malachite green (0.045% [w/v] in a 1% PVA solution) and sodium molybdate (4.8% [w/v] in 5 M HCl) at a ratio of 3:1. After 5 min, the absorbance at 625 nm was measured using a BMG LABTECH POLARstar Omega Microplate Reader. The background absorbance (same reaction without addition of MurA) was subtracted from the measured absorbance values. The reaction was prepared in triplicates and IC₅₀ values were determined using at least eight concentrations of the inhibitors. The data were fitted to a dose-response curve using OriginPro 2020. Ligand efficiency data for some selected compounds are listed in Supporting Information: Table S2.

4.2.5 | Antibacterial activities

Growth inhibition of *E. coli* Δ tolC and *S. aureus* (Newman strain) was investigated for all compounds with a maximal DMSO concentration of 1% as previously described.^[51] The final compound concentrations prepared from serial dilutions ranged from 3.125 to 100 μ M. OD values were determined at 600 nm after addition of the compounds and again after incubation at 50 rpm and 37°C for 16 h in 96-well plates using a POLARstar Omega Microplate Reader (BMG LAB-TECH). Experiments were performed at least twice. LB broth was used for *E. coli*, and Müller Hinton medium was used for *S. aureus*.

4.2.6 | Fluorescence binding assay

Fluorescence spectra were measured at rt and recorded on a FP-8300 JASCO spectrometer (wavelength accuracy \pm 1.5 nm) using quartz glass cuvettes (precision cuvettes made of quartz glass Model FP-1004, JASCO parts center). The measurements were conducted in 50 mM phosphate buffer (pH 6.9) with 1 mM DTT. The fluorescence was measured at an excitation wavelength of 366 nm and the emission spectra were recorded between 375 and 700 nm. The concentrations of both WT *E. coli* and *E. cloacae* MurA were 140 μ g/mL. The concentrations of ANS and compounds **11** and **26** were 100, 10, and 1 μ M, respectively. The spectra were recorded 5 min after addition of the ligand.

4.3 | Molecular docking

Molecular modeling and docking studies were performed using MOE 2010 as previously described.^[52]

ACKNOWLEDGMENTS

We would like to thank Professor Gregor Jung (Saarland University) for access to his spectrofluorometer.

CONFLICTS OF INTEREST STATEMENT

The authors declare no conflicts of interest.

ORCID

Matthias Engel  <http://orcid.org/0000-0001-5065-8634>

Christian Ducho  <http://orcid.org/0000-0002-0629-9993>

REFERENCES

- [1] L. Chang, E. Wen, J. Hung, C. Chang, *J. Protein Chem.* **1994**, *13*, 635.
- [2] L. Stryer, *J. Mol. Biol.* **1965**, *13*, 482.
- [3] E. Schönbrunn, S. Eschenburg, K. Luger, W. Kabsch, N. Amrhein, *Proc. Natl. Acad. Sci. USA.* **2000**, *97*, 6345.
- [4] N. Wang, E. B. Faber, G. I. Georg, *ACS Omega* **2019**, *4*, 18472.
- [5] E. Daniel, G. Weber, *Biochemistry* **1966**, *5*, 1893.
- [6] Z. Zuo, H. Fan, J. Guo, W. Zhou, L. Li, *Protein J.* **2012**, *31*, 585.
- [7] N. D. Younan, J. H. Viles, *Biochemistry* **2015**, *54*, 4297.

- [8] K. Kakuda, K. Yamaguchi, K. Kuwata, R. Honda, *Biochem. Biophys. Res. Commun.* **2018**, 506, 81.
- [9] Y. Goto, A. L. Fink, *Biochemistry* **1989**, 28, 945.
- [10] D. Matulis, R. Lovrien, *Biophys. J.* **1998**, 74, 422.
- [11] O. K. Gasymov, B. J. Glasgow, *Biochim. Biophys. Acta Prot. Proteom.* **2007**, 1774, 403.
- [12] D. M. Togashi, A. G. Ryder, *J. Fluoresc.* **2008**, 18, 519.
- [13] S. Betzi, R. Alam, M. Martin, D. J. Lubbers, H. Han, S. R. Jakkaraaj, G. I. Georg, E. Schönbrunn, *ACS Chem. Biol.* **2011**, 6, 492.
- [14] R. León, J. I. Murray, G. Cragg, B. Farnell, N. R. West, T. C. S. Pace, P. H. Watson, C. Bohne, M. J. Boulanger, F. Hof, *Biochemistry* **2009**, 48, 10591.
- [15] M. Hirose, S. Sugiyama, H. Ishida, M. Niiyama, D. Matsuoka, T. Hara, E. Mizohata, S. Murakami, T. Inoue, S. Matsuoka, M. Murata, *J. Synchrotron Radiat.* **2013**, 20, 923.
- [16] M. R. Groves, I. B. Müller, X. Kreplin, J. Müller-Dieckmann, *Acta Crystallogr. D. Biol. Crystallogr.* **2007**, 63, 526.
- [17] S. Sack, Z. Dauter, C. Wanke, N. Amrhein, E. Mandelkow, E. Schönbrunn, *J. Struct. Biol.* **1996**, 117, 73.
- [18] E. Schönbrunn, S. Sack, S. Eschenburg, A. Perrakis, F. Krekel, N. Amrhein, E. Mandelkow, *Structure* **1996**, 4, 1065.
- [19] T. Skarzynski, A. Mistry, A. Wonacott, S. E. Hutchinson, V. A. Kelly, K. Duncan, *Structure* **1996**, 4, 1465.
- [20] J. Y. Zhu, Y. Yang, H. Han, S. Betzi, S. H. Olesen, F. Marsilio, E. Schönbrunn, *J. Biol. Chem.* **2012**, 287, 12657.
- [21] E. D. Brown, J. L. Marquardt, J. P. Lee, C. T. Walsh, K. S. Anderson, *Biochemistry* **1994**, 33, 10638.
- [22] D. H. Kim, W. J. Lees, K. E. Kempell, W. S. Lane, K. Duncan, C. T. Walsh, *Biochemistry* **1996**, 35, 4923.
- [23] C. Wanke, N. Amrhein, *Eur. J. Biochem.* **1993**, 218, 861.
- [24] S. Mizyed, A. Oddone, B. Byczynski, D. W. Hughes, P. J. Berti, *Biochemistry* **2005**, 44, 4011.
- [25] L. L. Silver, *Cold Spring Harbor Perspect. Med.* **2017**, 7, a025262.
- [26] C. Marquès, V. Collin, C. Franceschi, N. Charbonnel, S. Chatellier, C. Forestier, *J. Antibiot.* **2020**, 73, 91.
- [27] S. Eschenburg, M. Priestman, E. Schönbrunn, *J. Biol. Chem.* **2005**, 280, 3757.
- [28] J. L. Marquardt, E. D. Brown, W. S. Lane, T. M. Haley, Y. Ichikawa, C. H. Wong, C. T. Walsh, *Biochemistry* **1994**, 33, 10646.
- [29] P. Liu, S. Chen, Z. Wu, M. Qi, X. Li, C. Liu, *J. Glob. Antimicrob. Res.* **2020**, 22, 238.
- [30] A. Sorlozano-Puerto, I. Lopez-Machado, M. Albertuz-Crespo, L. J. Martinez-Gonzalez, J. Gutierrez-Fernandez, *Antibiotics* **2020**, 9, 534.
- [31] Z. Fu, Y. Ma, C. Chen, Y. Guo, F. Hu, Y. Liu, X. Xu, M. Wang, *Front. Microbiol.* **2016**, 6, 1544.
- [32] K. L. Fillgrove, S. Pakhomova, M. R. Schaab, M. E. Newcomer, R. N. Armstrong, *Biochemistry* **2007**, 46, 8110.
- [33] J. E. Suárez, M. C. Mendoza, *Antimicrob. Agents Chemother.* **1991**, 35, 791.
- [34] P. Arca, *J. Antimicrob. Chemother.* **1997**, 40, 393.
- [35] P. Arca, C. Hardisson, J. E. Suárez, *Antimicrob. Agents Chemother.* **1990**, 34, 844.
- [36] B. A. Bernat, L. T. Laughlin, R. N. Armstrong, *Biochemistry* **1997**, 36, 3050.
- [37] T. Horii, T. Kimura, K. Sato, K. Shibayama, M. Ohta, *Antimicrob. Agents Chemother.* **1999**, 43, 789.
- [38] J. L. Marquardt, D. A. Siegele, R. Kolter, C. T. Walsh, *J. Bacteriol.* **1992**, 174, 5748.
- [39] A. Steinbach, A. J. Scheidig, C. D. Klein, *J. Med. Chem.* **2008**, 51, 5143.
- [40] A. Bachelier, R. Mayer, C. D. Klein, *Bioorg. Med. Chem. Lett.* **2006**, 16, 5605.
- [41] C. J. Dunsmore, K. Miller, K. L. Blake, S. G. Patching, P. J. F. Henderson, J. A. Garnett, W. J. Stubbings, S. E. V. Phillips, D. J. Palestrant, J. D. L. Angeles, J. A. Leeds, I. Chopra, C. W. G. Fishwick, *Bioorg. Med. Chem. Lett.* **2008**, 18, 1730.
- [42] K. Miller, C. J. Dunsmore, J. A. Leeds, S. G. Patching, M. Sachdeva, K. L. Blake, W. J. Stubbings, K. J. Simmons, P. J. F. Henderson, J. De Los Angeles, C. W. G. Fishwick, I. Chopra, *J. Antimicrob. Chemother.* **2010**, 65, 2566.
- [43] T. Scholz, C. L. Heyl, D. Bernardi, S. Zimmermann, L. Kattner, C. D. Klein, *Bioorg. Med. Chem.* **2013**, 21, 795.
- [44] C.-M. Chang, J. Chern, M.-Y. Chen, K.-F. Huang, C.-H. Chen, Y.-L. Yang, S.-H. Wu, *J. Am. Chem. Soc.* **2015**, 137, 267.
- [45] J. D. McGivan, J. B. Chappell, *Biochem. J.* **1970**, 116, 37.
- [46] E. Schönbrunn, S. Eschenburg, F. Krekel, K. Luger, N. Amrhein, *Biochemistry* **2000**, 39, 2164.
- [47] E. Schonbrunn, D. I. Svergun, N. Amrhein, M. H. J. Koch, *Eur. J. Biochem.* **1998**, 253, 406.
- [48] E. M. Kosower, H. Kanety, *J. Am. Chem. Soc.* **1983**, 105, 6236.
- [49] In Silico Bioinformatics Resources, University of Düsseldorf ligation Calculator, http://www.insilico.uni-duesseldorf.de/Lig_Input.html
- [50] R. K. Fathalla, W. Fröhner, C. D. Bader, P. D. Fischer, C. Dahlem, D. Chatterjee, S. Mathea, A. K. Kiemer, H. Arthanari, R. Müller, M. Abdel-Halim, C. Ducho, M. Engel, *J. Med. Chem.* **2022**, 65, 14740.
- [51] A. P. Spork, M. Büschleb, O. Ries, D. Wiegmann, S. Boettcher, A. Mihalyi, T. D. H. Bugg, C. Ducho, *Chem. Eur. J.* **2014**, 20, 15292.
- [52] A. K. Elhady, M. Abdel-Halim, A. H. Abadi, M. Engel, *J. Med. Chem.* **2017**, 60, 5377.

SUPPORTING INFORMATION

Additional supporting information can be found online in the Supporting Information section at the end of this article.

How to cite this article: R. K. Fathalla, M. Engel, C. Ducho, *Arch. Pharm.* **2023**;356:e2300237.
<https://doi.org/10.1002/ardp.202300237>